Aalborg Universitet

Impact of lifetime model selections on the reliability prediction of IGBT modules in modular multilevel converters

Zhang, Yi; Wang, Huai; Wang, Zhongxu; Yang, Yongheng; Blaabjerg, Frede

Impact of Lifetime Model Selections on the Reliability Prediction of IGBT Modules in Modular Multilevel Converters

Yi Zhang, Huai Wang, Zhongxu Wang, Yongheng Yang, Frede Blaabjerg
Center Of Reliable Power Electronics (CORPE)
Department of Energy Technology, Aalborg University
yiz@et.aau.dk; hwa@et.aau.dk; zho@et.aau.dk; yoy@et.aau.dk; fbl@et.aau.dk

Abstract—Power cycling in semiconductor modules contributes to repetitive thermal-mechanical stresses, which in return accumulate as fatigue on the devices, and challenge the lifetime. Typically, lifetime models are expressed in number-of-cycles, within which the device can operate without failures under predefined conditions. In these lifetime models, thermal stresses (e.g., junction temperature variations) are commonly considered. However, the lifetime of power devices involves in cross-disciplinary knowledge. As a result, the lifetime prediction is affected by the selected lifetime model. In this regard, this paper benchmarks the most commonly-employed lifetime models of power semiconductor devices for offshore Modular Multilevel Converters (MMC) based wind farms. The benchmarking reveals that the lifetime model selection has a significant impact on the lifetime estimation. The use of analytical lifetime models should be justified in terms of applicability, limitations, and underlying statistical properties.

Index Terms—Insulated gate bipolar transistor (IGBT), lifetime model, modular multilevel converter, power semiconductor module, reliability.

I. INTRODUCTION

Modular Multilevel Converters (MMCs) are promising high-power Voltage-Source Converters (VSCs) for wind farms [1]. In the MMC offshore wind systems, a large number of IGBT modules are used. According to an industrial survey in 2009 [2], IGBT modules are one of the most vulnerable components in electrical system. To support design and operational management, it is important to predict the lifetime of power devices.

As the advantages of MMCs (i.e., modularity, redundancy, etc.), many existing studies about MMC have been devoted to the modeling and control [3]. The study about the lifetime of power devices in the MMC is rarely seen although reliability is one of the major concerns during the design and operational management. For instance, in order to optimize the semi-conductor device utilization, reliability, redundancy design, capital cost and periodic preventive maintenance schedule, models based on conventional reliability metrics constant failure rate and the corresponding mean-time-between-failures (MTBF) has been used in [4], [5], [6]. However, the constant failure rate model is found to be inappropriate in practice [7]. The neglect of wear-out stage of power devices may be misleading. Therefore, a time-varied failure rate model is
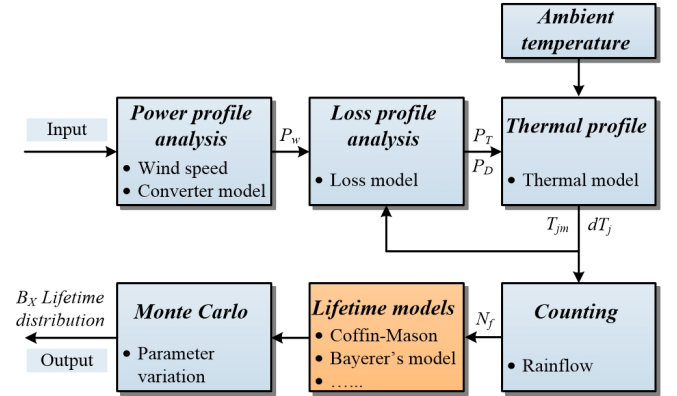

Fig. 1. Mission-profile-based approach to assessing the reliability of power electronics systems (e.g., an MMC wind power system).

essential to lifetime prediction of power electronic converters, including MMCs.

In addition, a mission profile based lifetime estimation model has been proposed for the IGBT modules of MMC systems [8], but the adoption of a specific lifetime model is not discussed. Considering the specific limitation and effective boundary for different lifetime models, the indiscriminate use of lifetime models is not recommended. Nevertheless, beyond MMC applications, this is neither addressed in many other cases, e.g., onshore and offshore wind turbine systems (WTS) [9], photovoltaic (PV) systems [10], air conditioners and pump systems. In other words, the impact of lifetime model selection remains unclear. Therefore, this paper is focused on the benchmarking of the most commonly-adopted lifetime models of IGBT devices in MMC systems.

The lifetime prediction methods of IGBT modules can be classified into two categories. The first one is based on analytical models developed from accelerated lifetime testing data [11], [12]. The second category is based physics-of-failure (PoF) lifetime models, but it is still limited due to the lack of detailed information of the materials and geometries of IGBT modules. Thus, the discussion of this paper is limited to analytical models only, where the mission profiles (i.e., wind speed and ambient temperature) are also considered in the analysis as demonstrated in Fig. 1.
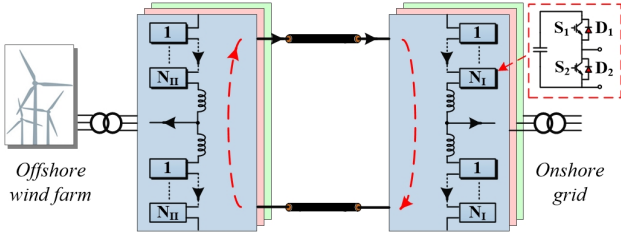
Fig. 2. System structure of an offshore MMC wind farm.

In this paper, the system description and mission profile are discussed in Section II. Section III deals with the analytical calculation of the loading profile, loss profile, thermal profile and thermal cycles using an annual mission profile recorded from a real-field wind farm. Section IV estimates and compares the impact of different lifetime models on the reliability prediction of MMC systems. Concluding remarks are drawn based on simulation at last.

II. SYSTEM DESCRIPTION AND MISSION PROFILE

To illustrate the lifetime estimation procedure, an offshore MMC wind power transmission system as shown in Fig. 2 is considered in this paper, where both the wind farm-side and the grid-side converters are three-phase MMCs. In each phase of the MMC, there are 24 identical half-bridge Sub-Modules (SMs), and each SM consists of two IGBT power devices from ABB 5SNA 1200E450350, that is, the upper $IGBT_1$ (i.e., IGBT chip S_1 and diode D_1) and lower $IGBT_2$ (S_2 and D_2) as shown in Fig. 2. Then, the system specifications are listed in Table I. An annual mission profile (i.e., wind speed and ambient temperature) is adopted and the data is one hour averaged at 80-meter hub height as shown in Fig. 3. The data was collected from a wind farm located at the latitude of $54.25°$ and the longitude of $8.20°$. The hub speed belongs to the IEC Wind Class I with an average wind speed of 8.5-10 m/s. For the wind farm, ten V90 wind turbines [13] with a 3-MW rated power are chosen in the case.

III. MISSION PROFILE TRANSLATION TO POWER CYCLING

In IGBT modules, thermal cycling contributes to accumulative fatigue and thus a progressive wear-out of the device. Thus, in order to analyze the impact of lifetime models on the reliability prediction, mission profiles have to be translated into thermal loading.

A. Power Profile

To evaluate the loss distribution, the power loading profile of the MMC should be calculated firstly. The wind profile shown in Fig. 3 will be fed into the WT model provided by the manufacturer [13] to calculate the power production profile. All WTs are assumed operating under identical conditions. Following, the annual power production from a WT corresponding to the wind speed is shown in Fig. 4. A large fluctuation is observed during the year. Finally, the total power
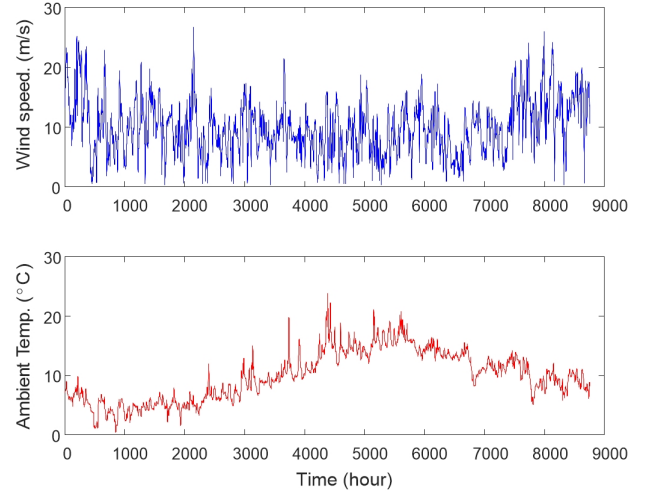

Fig. 3. One-year mission profile of wind speed and ambient temperature from an offshore wind farm (one hour average per data).
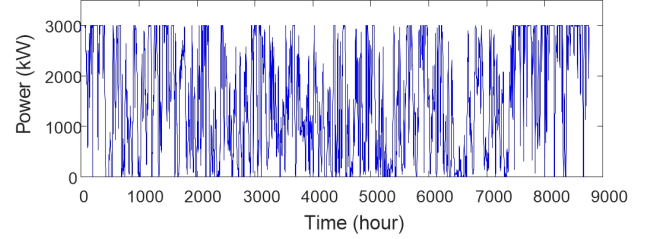

Fig. 4. Annual produced power by each wind turbine.

production from the wind farm can be obtained by multiplying the number of wind turbines (i.e., 10).

B. Loss Profile

Compared with two- or three-level VSCs, the power loss calculation of the MMC are relatively complicated. A Phase Shifted Carrier Pulse Width Modulation (PSC-PWM) scheme is adopted here. The working principle along with its power loss calculations has been introduced in [8], where the operational principle of the i_{th} SM in the MMC can be divided into four stages depending on the gate signal of the SM $g_{p(n),i,k}$ (i is the i-th SM in each arm; $k = a$, b, c; p = upper arm, n = lower arm; g_{S1}, g_{S2}, g_{D1}, g_{D2} denoting the on-off state of S_1, S_2, D_1 and D_2 respectively). The current direction $i_{p(n),k}$ and the operational states are summarized in Table II.

According to [14], the average switching losses of power devices (IGBTs or diodes) can be obtained as

$$P_{sw\_avg} = f_0 \cdot \int_0^{1/f_0} P_{sw\_inst}(t)dt \qquad (1)$$

where the instantaneous switching loss P_{sw_inst} of the power devices can be calculated by

$$P_{sw\_inst}(t) = f_{sw} \cdot E_{sw}\left(i_c(t), T_j\right) \cdot (U_{SM}/U_{ref})^{K_v} \qquad (2)$$

in which U_{ref} is the commutated voltage from data-sheet, f_{sw} is the switching frequency, and f_0 is the fundamental

frequency, and $E_{sw}(i_c(t), T_j)$ is the switching energy per pulse, which is a function of the collector current $i_c(t)$ of power devices and junction temperature T_j. It is expressed as

$$E_{sw}\left(i_c(t), T_j\right) = E_{sw}\left(i_c(t), T_{ref}\right) \cdot \left[1 + K_T \cdot (T_j - T_{ref})\right] \tag{3}$$

Similarly, the average condition loss P_{cond_avg} can be calculated as

$$P_{cond\_avg} = f_0 \cdot \int_0^{1/f_0} P_{cond\_inst}(t)dt \tag{4}$$

where the instantaneous conduction loss P_{cond_inst} can be obtained as

$$P_{cond\_inst}(t) = u_{cond}\left(i_c(t), T_j\right) \cdot i_c(t) \cdot M(m, t) \tag{5}$$

where the duty ratio $M(m, t)$ is a function of modulation index m, and the conduction voltage $u_{cond}\left(i_c(t), T_j\right)$ of power devices can be founded in datasheet, and it can be analytically represented by

$$u_{cond}\left(i_c(t), T_j\right) = U_{cond0}\left(T_{ref}\right) \cdot \left[1 + K_{T2} \cdot (T_j - T_{ref})\right]$$
$$+ i_c(t) \cdot \left[r_{cond}\left(T_{ref}\right) + K_{T3} \cdot (T_j - T_{ref})\right] \tag{6}$$

in which K_{T1}, K_{T2}, K_{T3}, K_v, U_{cond0}, r_{cond} are coefficients that can be obtained by fitting the parameters to the corresponding curves in data-sheet.

From the above analysis, it can be seen that the power loss is affected by the loading current, conduction voltage, switching frequency, fundamental frequency, conduction time, and modulation strategy. As the PSC-PWM strategy is used, the switching frequency, fundamental frequency and the conduction time are the same for all modules in each fundamental period. Moreover, the arm current $i_{p(n),k}$ and the capacitor voltage $U_{SM,p(n),i,k}$ in the six arms are the same in each fundamental period, only with different phase-shifted angles. Thus, the power losses in each fundamental period will be the same among those in SMs. Finally, the power losses of the IGBT modules are obtained, as illustrated in Fig. 5.

C. Thermal Profile

Based on the loss profile in Fig. 5, the thermal stress of the power semiconductor devices can be obtained. A Foster model is employed as shown in Fig. 5, where the thermal impedance that determines the junction temperature consists of the power module itself (from junction to baseplate), the Thermal Interface Material (TIM), and the cooling part. In this case, the liquid temperature of the water-cooled heat-sink is set as 40 °C, and the maximum junction temperature is set at 115 °C. The heatsinks of both IGBTs in a SM have an identical design.

Accordingly, the thermal profile of the IGBT modules can be obtained. The junction temperatures T_j of both IGBT chips, and the baseplate temperatures T_c are shown in Fig. 5. Additionally, it can also be seen in Fig. 5 that fluctuations of T_j and T_c in S_2 are more intensive with large amplitudes than S_1, which implies the inherent thermal unbalance in the SM of the MMC.

D. Power Cycle Counting

When the thermal profile is obtained, a rainflow counting method [15] has to be applied in order to convert the random thermal profile to the regular thermal cycle, which are more suitable for lifetime models. The temperature swing amplitude ΔT_j and the mean temperature T_{jm} of the thermal cycles have strong impacts on the lifetime of power devices. The counting results from the long-term thermal loading in Fig. 5 is shown in Fig. 6. It can be seen that the number of cycles in S_2 is far more than that in S_1, which reflects the intensive fluctuations of thermal profiles in Fig. 5. Furthermore, the rainflow results of the baseplate temperatures of both IGBTs and diodes can be obtained in a similar way.

IV. BENCHMARKING LIFETIME MODELS

This section aims to estimate the lifetime of the MMC and compares the most commonly-employed lifetime models, as shown in Table III. The first model – Coffin Manson model [11] is the simplest, only considering the amplitude of the temperature swing. The other models add more parameters, such as the elastic strain ΔT_0 [7], absolute temperature (mean temperature T_m or minimum temperature $T_{\min}$), and power-on-time t_{on}, etc. Moreover, E_a and k_B denote activation energy and the Boltzmann constant, respectively [16]. Parameters A, n, β_2, β_3, β_4, β_5 and β_6 are obtained according to the aging data provided by the manufacturer [17]. Noted that the three factors (I current per bond wire, V blocking voltage of the chip, D diameter of the bond wire) can be assumed constant, since a fixed power module is utilized in the case study.

In order to compare different lifetime models, a lookup table method based on the aging data from the manufacturer [17] has been established as the benchmark. The lifetime results from the selected lifetime models listed in Table III are compared with the benchmark, where S_1 and D_1 represent IGBT$_1$ and
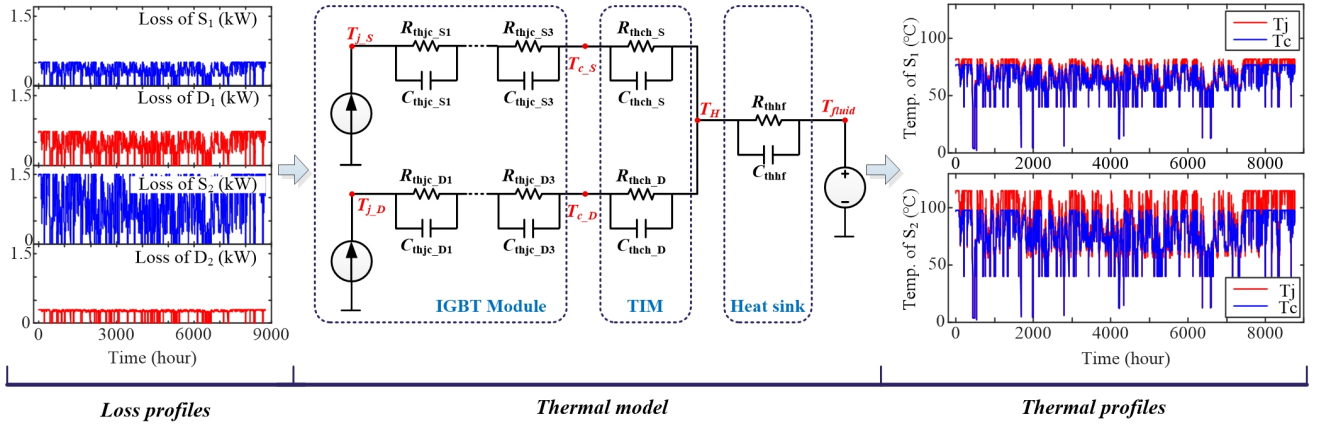
Fig. 5. Power losses of the devices in an SM of the MMC and its annual thermal profiles of both IGBTs in the SM in respect to the thermal model.
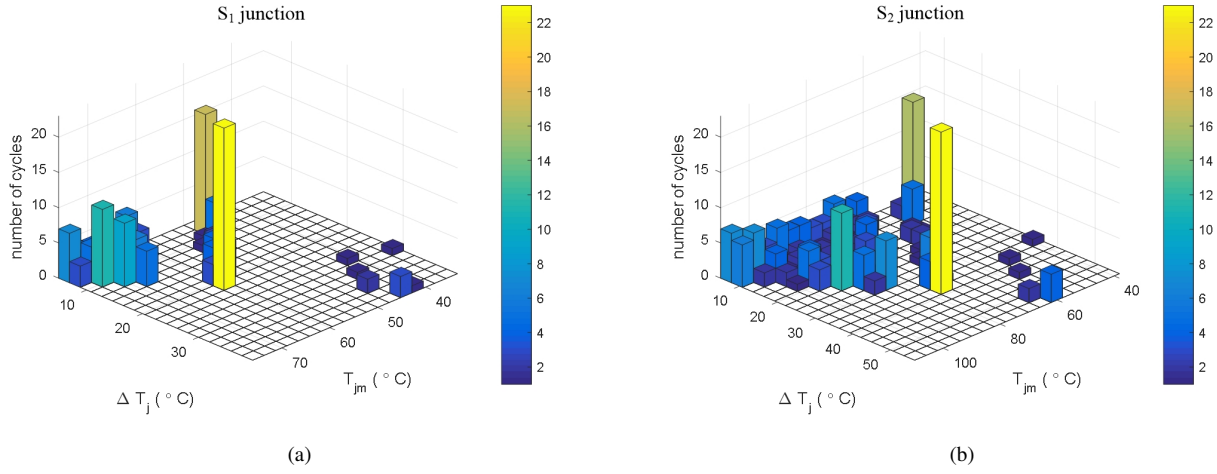

Fig. 6. Rainflow counting results of one year thermal profile. (a) IGBT$_1$ and (b) IGBT$_2$.

TABLE III
THE COMMONLY-EMPLOYED CYCLE TO FAILURE MODELS (ANALYTICAL MODELS).

No.	Model Name	Analytical Lifetime Models	Major impacts
1	Coffin-Manson Model [11]	$N_f = A \Delta T^{-n}$	only amplitude of temperature
2	General Coffin-Manson Model [7]	$N_f = A (\Delta T - \Delta T_0)^{-n}$	Model 1 + elastic region
3	Modified Coffin-Manson Model [16]	$N_f = A \Delta T^{-n} \cdot \exp\left(\frac{E_a}{k_B T_m}\right)$	Model 1 + absolute temperature
4	General Modified Coffin-Manson Model	$N_f = A (\Delta T - \Delta T_0)^{-n} \cdot \exp\left(\frac{E_a}{k_B T_m}\right)$	Model 1 + absolute temperature + elastic region
5	Bayerer's Model [12]	$N_f = A \Delta T^{-n} \cdot \exp\left(\frac{\beta_2}{T_{\min}}\right) t_{on}^{\beta_3} I^{\beta_4} V^{\beta_5} D^{\beta_6}$	Model 3 + power-on-time
6	General Bayerer's Model	$N_f = A (\Delta T - \Delta T_0)^{-n} \cdot \exp\left(\frac{\beta_2}{T_{\min}}\right) t_{on}^{\beta_3} I^{\beta_4} V^{\beta_5} D^{\beta_6}$	Model 3 + power-on-time + elastic region

its diode in the SM of the MMC, and S_2 and D_2 are IGBT$_2$ and its diode. The results are shown in Fig. 7.

The manufacturer provided aging data is the B$_{10}$ lifetime, which is defined as the number of cycles where 10 % of the modules of a population fail. Then, as shown in Fig. 7, the consumed B$_{10}$ lifetime of IGBT$_2$ is larger than IGBT$_1$ no matter which lifetime models are employed. It is due to the intensive fluctuations of thermal profiles in Fig. 5. However, taking the lifetime results of the chip solder in IGBT$_1$ as an example,

labeled as S$_1$_CS in Fig. 7, the benchmark is 1.129×10^{-5}, which is smaller than the results from analytical models. When the Coffin-Manson (Model 1) is adopted, the result is nearly 10 times of the benchmark, since only the temperature variation amplitude is considered in this model. When the elastic strain range ΔT_0 is considered, as in Model 2, the consumed lifetime of S$_1$_CS is approaching the benchmark. It implies that a large number of small temperature variations ΔT also introduce fatigue, but the impact is assumed negligible in most of
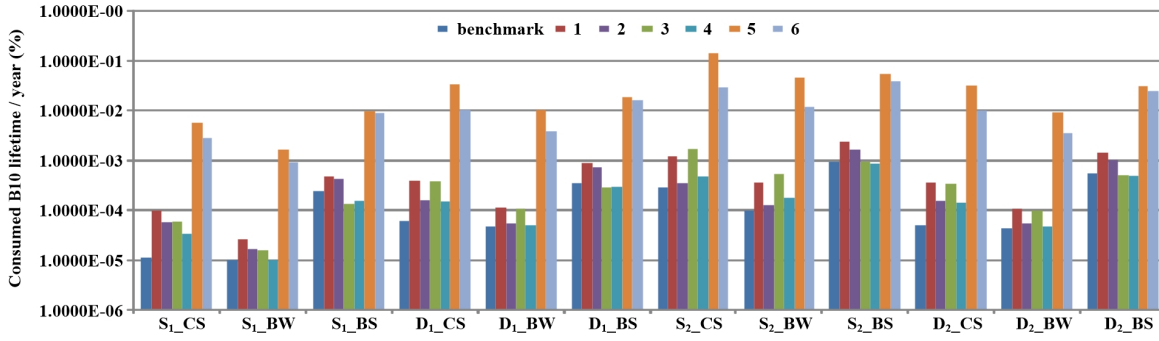
Fig. 7. Consumed B_{10} lifetime of both IGBTs and diodes in an SM of the MMC according to the aging data from the manufacturer and six different lifetime models (S_1 and D_1 mean the $IGBT_1$ and its diode in a SM, and S_2 and D_2 are the $IGBT_2$ and its diode, CS – chip solder, BW – bond wire, and BS – base plate solder).
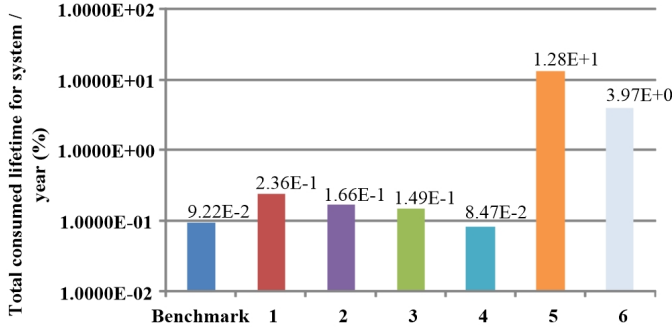

Fig. 8. Total lifetime consumed in the entire MMC system where the lifetime consumption from the six different lifetime models is compared.

the prior-art study. In Model 3, the absolute temperature is also introduced into the lifetime estimation. It accounts for the difference whether the same temperature variation ΔT is performed in different minimum temperature or maximum temperature. The result of Model 3 is thus more accurate, reflecting the influence of the absolute temperature. Moreover, when both ΔT_0 and T_m are considered, as in Model 4, its prediction is further improved. However, when the power-on-time is introduced into the lifetime Models 5 and Model 6, larger errors are observed than the benchmark. This is due to the study case based on the wind profile with a time step of one hour. The power-on-time of the thermal profile is one hour at least that has been out of the effective range of t_{on}. In all, the lifetime model selection has a significant impact on the lifetime estimation. The use of analytical lifetime models should be justified in terms of applicability, limitations, and underlying statistical properties.

Nevertheless, consumers more concern about the lifespan of the entire system. The total lifetime consumed per year for the entire MMC is shown in Fig. 8, where the MMC consists of 72 SMs (144 IGBT modules). The values from the benchmark and Model 4 are very close. Thus, it can be concluded that the elastic range ΔT_0 and absolute temperature have significant impacts on the lifetime estimation. However, the power-on-time t_{on} should be carefully considered.

In this paper, the provided aging data of the IGBT module is based on B_{10} data. If B_5 and B_1 are necessary, which are the total number of cycles during which 5 % and 1 % of the modules fails, the manufacturer provided the factors k_5 = 0.90 and k_1 = 0.70, respectively [17]. It means that B_5 and B_1 lifetime data can be calculated by multiplying the B_{10} lifetime with corresponding factors. Moreover, the aging data is determined by the Weibull distribution. The end-of-life distribution of the MMC (only considering the failures of power semiconductors due to fatigue) is shown in Fig. 9. It can be noted that the estimated lifetime of the MMC is 10.8 years within 10% failure of IGBTs in the Benchmark. However, the results of Model 1 to Model 3 are 4.24 years, 6.02 years, and 6.71 years, which takes into account the amplitude of temperature, the elastic region, and the absolute temperature, respectively. When all these factors are considered into Model 4, the predicted lifetime is 11.8 years, which is closed to the benchmark result. It reveals that the elastic region and the absolute temperature have a significant impact on the lifetime prediction. On the other hand, the predicted B_{10} lifetime based on Model 5 and Model 6 is smaller than 1 year, which is far away from the benchmark result. Although all three factors mentioned above have been considered in the two Models, the results have large difference since the power-on-time is beyond its effectiveness range. Therefore, the lifetime model selection is recommended to consider various factors as well as its testing range.

V. CONCLUSION

This paper has compared the most commonly-used analytical lifetime models for lifetime prediction of IGBT devices in MMC systems, where an annual mission profile is considered. The translation from the mission profile to the power profile, loss profile, and thermal profile is conducted. Accordingly it enables the rainflow counting. That is, the random thermal stresses are converted to regular thermal cycles. The resultant thermal cycles have then been applied to predict the lifetime of the IGBT devices, where the results from six lifetime models are compared with the tested aging data. The benchmarking reveals the most widely accepted Coffin-Manson model has
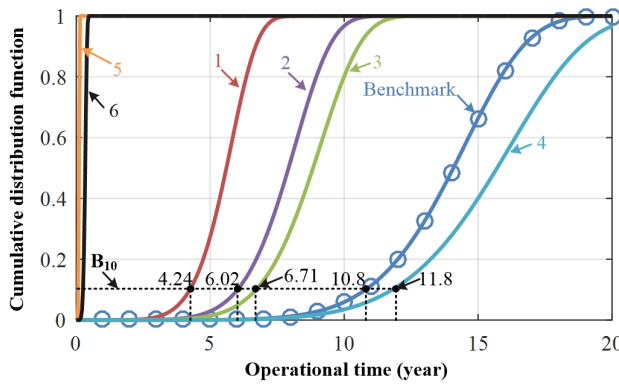
Fig. 9. End-of-life cumulative distribution function of the MMC due to the fatigue of power semiconductors

a large error. Considerations of the elastic deformation with small temperature swings ΔT and the absolute temperature are beneficial to the lifetime estimation. However, the selection of the power-on-time should consider the effective range of t_{on}.

REFERENCES

[1] M. A. Perez, S. Bernet, J. Rodriguez, S. Kouro, and R. Lizana, "Circuit topologies, modelling, control schemes and applications of modular multilevel converters," *IEEE Trans. Power Electron.*, vol. 30, no. 1, pp. 4–17, Jan. 2015.

[2] S. Yang, A. Bryant, P. Mawby, D. Xiang, L. Ran, and P. Tavner, "An industry-based survey of reliability in power electronic converters," *IEEE Trans. Ind. Appl.*, vol. 47, no. 3, pp. 1441–1451, May/Jun. 2011.

[3] M. Hagiwara and H. Akagi, "Control and experiment of pulsewidth-modulated modular multilevel converters," *IEEE Trans. Power Electron.*, vol. 24, no. 7, pp. 1737–1746, Jul. 2009.

[4] J. Xu, P. Zhao, and C. Zhao, "Reliability analysis and redundancy configuration of mmc with hybrid submodule topologies," *IEEE Trans. Power Electron.*, vol. 31, no. 4, pp. 2720–2729, Apr. 2016.

[5] K. Nieradzinska, C. MacIver, S. Gill, G. A. Agnew, O. Anaya-Lara, and K. R. W. Bell, "Optioneering analysis for connecting Dogger Bank offshore wind farms to the GB electricity network," *Renewable Energy*, vol. 91, pp. 120–129, 2016.

[6] B. Wang, X. Wang, Z. Bie, P. D. Judge, X. Wang, and T. C. Green, "Reliability model of mmc considering periodic preventive maintenance," *IEEE Trans. Power Del.*, vol. 8977, no. c, pp. 1–1, Aug. 2016.

[7] H. Wang, K. Ma, and F. Blaabjerg, "Design for reliability of power electronic systems," in *Proc. IECON 38th Annual Conf. IEEE Ind. Electron. Society*, 2012, pp. 33–44.

[8] H. Liu, K. Ma, Z. Qin, P. C. Loh, and F. Blaabjerg, "Lifetime estimation of MMC for offshore wind power HVDC application," *IEEE J. Emerg. Sel. Topics Power Electron.*, vol. 4, no. 2, pp. 504–511, Sep. 2016.

[9] K. Ma, M. Liserre, F. Blaabjerg, and T. Kerekes, "Thermal loading and lifetime estimation for power device considering mission profiles in wind power converter," *IEEE Trans. Power Electron.*, vol. 30, no. 2, pp. 590–602, Mar. 2015.

[10] S. B. Kjaer, J. K. Pedersen, and F. Blaabjerg, "A review of single-phase grid-connected inverters for photovoltaic modules," *IEEE Trans. Ind. Appl.*, vol. 41, no. 5, pp. 1292–1306, Sep. 2005.

[11] S. S. Manson and T. Dolan, "Thermal stress and low cycle fatigue," *J. Applied Mechanics*, vol. 33, p. 957, 1966.

[12] R. Bayerer, T. Herrmann, T. Licht, J. Lutz, and M. Feller, "Model for power cycling lifetime of IGBT modules - various factors influencing lifetime," in *Proc. 5th Int. Conf. Integrated Power Electron. Systems*, Mar. 2008, pp. 1–6.

[13] "Vestas V90 3.0 MW data.pdf." [Online]. Available: https://www.vestas.com/

[14] K. Ma, M. Liserre, and F. Blaabjerg, "Operating and loading conditions of a three-level neutral-point-clamped wind power converter under various grid faults," *IEEE Trans. Ind. Appli.*, vol. 50, no. 1, pp. 520–529, Jun. 2014.

[15] A. Niesłony, "Determination of fragments of multiaxial service loading strongly influencing the fatigue of machine components," *Mechanical Systems and Signal Processing*, vol. 23, no. 8, pp. 2712–2721, 2009.

[16] A. Wintrich, N. Ulrich, T. Werner, and T. Reimann, *Application Manual Power Semiconductors*. Nuremberg, Germany: Semikron Int.GmbH, 2015.

[17] E. Özkol, S. Hartmann, and H. Duran, "Load-cycling capability of HiPak^{TM} IGBT modules 5SYA2043-03," Tech. Rep., 2012.